Chemical Engineering Journal 461 (2023) 141956

Contents lists available at ScienceDirect

Chemical Engineering Journal

journal homepage: www.elsevier.com/locate/cej

Countercurrent moving bed carbonator for CO_2 capture in decoupled calcium looping systems

J. Carlos Abanades, Yolanda A. Criado *, Roberto García

CSIC-INCAR, C/ Francisco Pintado Fe, 26, 33011 Oviedo, Spain

ARTICLE INFO

Keywords:
CO_2 capture
Moving bed
Carbonation

ABSTRACT

Calcium Looping can be a suitable technology to address the CO_2 capture from disperse flue gas sources, including shipping, by decoupling carbonation and calcination steps and by using the $CaCO_3$ as CO_2 transport media. In this work we present the design of a moving bed carbonator especially suited for these applications. The Ca-sorbent material (porous CaO or $Ca(OH)_2$ in the form of pebbles or pellets) is fed to the top of the reactor at ambient conditions and is preheated by the gases leaving the reactor. Then the carbonated solids leave the reactor at the bottom at a temperature close to that of the inlet gases. A basic countercurrent reactor model has been developed to identify operational windows and other suitable conditions to achieve optimum carbonation temperatures of 600–700 °C in the central carbonation zone of the reactor. Gas velocities of 1–3 m/s and solid residence times in the carbonation zone of between 2 and 13 h are needed to carbonate spheres of Ca-based materials of 1 to 2 cm up to its maximum conversion of 0.6 for CaO and 0.8 for $Ca(OH)_2$. The thermal and mechanical similarities of the proposed reactor with those of shaft kilns should accelerate the scaling up of this new reactor concept.

1. Introduction

Post-combustion Calcium Looping (CaL) systems have rapidly developed from a paper concept [1] to pilot systems reaching the MW scale when using circulating fluidized bed reactors [2–4]. CaL processes use CaO as a sorbent for the capture of CO_2 in carbonator reactors at temperatures around 650 °C, with a subsequent calcination step at temperatures over 900 °C (usually reached by oxy-combustion) to obtain a highly-concentrated stream of CO_2 while regenerating CaO. Since the calcination of $CaCO_3$ is a highly endothermic reaction (i.e. about 3.9 MJ/kg_{CO2}), CaL systems are only suitable when the high temperature heat flows available from the capture system (in particular from carbonation of CaO) are effectively integrated within the industrial process or used to generate power [5,6]. The CaL systems also offer strong material synergies and additional CO_2 avoidance by using the CaO-rich purges in the lime and cement industries (with process related emissions accounting respectively for 0.3 [7,8] and 2.5 Gt-CO_2/year [9]).

As it is the case for other CO_2 capture technologies, post-combustion CaL has been mainly conceived to decarbonize large stationary sources of CO_2 such as power [5,10–15] and cement plants [16–22]. However, the current drive to meet 1.5 ℃ targets [23] may require capture of CO_2 technologies to be applied in a wider variety of industries, where electrification and hydrogen may not be technically viable or economic in the long lifespan of current combustion plants. Examples of such industries are those relying on fuel combustion to reach high temperature environments that are inherent to their processes (e.g., glass, ceramics, special steels, waste-to-energy plants, paper mills, etc.). Some of these industrial sources of CO_2 may be conveniently located within large industrial clusters, so that they can find synergies to minimise the specific cost of CO_2 avoidance [24,25]. Nevertheless, there will be a number of disperse CO_2 emitting activities where these opportunities are simply not there. This is also the case for the current fleet of large ships used for freight transport (emitting up to 0.94 Gt-CO_2/year, mainly from heavy fuel combustion [26] and having lifetimes spanning well above 30 years) that demands for technological solutions to capture CO_2 [27].

The high molar density of carbon in $CaCO_3$ (contains 27.1 kmol CO_2/m^3, which would be equivalent to about 650 atm if it was an ideal gas at 20℃) offers a unique opportunity to provide CO_2 capture solutions for disperse sources of CO_2, by decoupling the capture step (i.e. the carbonation of CaO to $CaCO_3$) from the calcination stage and by exploiting the role of $CaCO_3$ as a CO_2 carrier in the CaL system. Indeed, such concept has been proposed as a strategy [28–30] to operate CaO

* Corresponding author.
E-mail address: yolanda.ac@incar.csic.es (Y.A. Criado).

https://doi.org/10.1016/j.cej.2023.141956
Received 22 December 2022; Received in revised form 10 February 2023; Accepted 14 February 2023
Available online 17 February 2023

Nomenclature

A_B	reactor cross-sectional area, m^2
C_{CO2}	CO_2 concentration, mol/m^3
Cp	specific heat, J/molK
D_{CO2}	CO_2 diffusion in air, m^2/s
D_{eff}	effective diffusion of CO_2 through the carbonated layer, m^2/s
d_p	particle diameter, m
E_{Carb}	carbonation efficiency
F	molar flow, mol/s
$f_{Ca,\ active}$	active fraction of Ca solids
L_{Carb}	length of the carbonation zone, m
q	heat flow, J/s
T	temperature, °C
t	time, s
T_{Max}	maximum temperature in the carbonation zone, °C
t_R	residence time of the solids in the carbonation zone, s
u_g	gas velocity, m/s
X	solids conversion with respect to their total volume
X_{CaCO3}	Ca molar conversion to $CaCO_3$
X_{Dehy}	$Ca(OH)_2$ molar conversion to CaO
Z_{Carb}	dimensionless countercurrent carbonator length
ΔH_{Carb}	CaO carbonation reaction enthalpy, J/mol
ΔH_{Dehy}	$Ca(OH)_2$ dehydration reaction enthalpy, J/mol
ΔP	pressure drop, bar
ε_B	bed porosity
ε_{Ca}	porosity of the Ca solids
ε_{Carb}	porosity of the carbonated layer according to equation (4)
ν_{CO2}	CO_2 molar fraction
ρ_{Ca}	molar density of Ca solids, mol/m^3
$\rho_{Ca,\ p}$	molar density of porous particles, mol/m^3
ρ_{CaCO3}	molar density of $CaCO_3$, mol/m^3
τ	tortuosity factor, calculated as $1/\sqrt{\varepsilon_{Ca}}$
τ_R	time for complete conversion, s

Subscripts

Ca	Ca sorbent
CO_2	CO_2 in the gas phase
eq	equilibrium
g	gas
in	reactor inlet conditions
out	reactor outlet conditions
r	reaction
s	solids
z	along the reactor length

carbonators to capture CO_2 in ships, using decarbonized lime stored on-board (but generated on-shore). The on-board formed $CaCO_3$ (and the unconverted CaO), can then be either stored or distributed in the ocean to enhance ocean liming [31]. Another example of decoupled Calcium Looping (d-CaL) system, is the proposed use of $Ca(OH)_2$ as a material for direct CO_2 capture from the atmosphere by its passive carbonation [32–35] or forced carbonation in a dedicated air contactor [36–39], transporting then the resulting $CaCO_3$ to centralized oxy-fired calciners [35]. Lisbona et al. [40] have also recently proposed the option of decoupled carbonator and calciner reactors in a CaL system to address capture CO_2 from disperse industrial sources. In this case the CaO is generated in the proximity of an oxy-fired cement plant and transported (at temperatures close to ambient) to an industrial site to be carbonated. The produced carbonate is then cooled down and transported back to the centralized oxy-calcination plant to extract the CO_2 by its calcination. The energy requirements in the proposed d-CaL system are larger than the standard integrated CaL because of the cooling and preheating requirements of the solids. But some emitters may still accept the inherent penalties of the d-CaL when no better alternative is available to decarbonize them.

In these type of d-CaL systems the choice of the most suitable carbonator reactor is far from obvious when considering the need to allow operations with a feed of $CaO/Ca(OH)_2$ at ambient temperature. Bubbling fluidized beds were the first reactor choice in CaL systems [1] because they facilitate the continuous solid circulation between calciner and carbonator. Circulating fluidized bed carbonators were introduced to accommodate the large gas velocity, solid circulation and solid make up flow requirements in CaL systems for large scale power plants [5,41]. Entrained carbonators have been also developed recently for integrated applications of CaL to cement plants [42] and are entering large pilot demonstration scale within the Cleanker project [22,43]. In all these three reactor systems, a continuous circulation of high temperature solids is established between carbonator and calciner to achieve maximum energy efficiencies while keeping the carbonator at optimum temperatures (i.e., around 650 C) to facilitate energy recovery and to avoid the lower carbonation conversions observed at modest temperatures [44]. Although there is no fundamental reason to prevent the use of fluidized or entrained bed carbonators in d-CaL systems, the need of extensive ancillary equipment for solid handling and heat recovery (i.e. cyclones, energy recovery subsystems, flue gas clean up devices, solid handling for the carbonated solids leaving the carbonator at high temperature, etc.) is likely to increase cost and/or energy inefficiencies in d-CaL systems. Furthermore, even if such complete set-up could be justified in on-shore d-CaL applications, it would be most likely uneconomic when the system needs to be installed on-board of a ship.

To address this challenge, we propose in this work the use of a novel reactor for carbonation by operating it in countercurrent mode [38]. We demonstrate that such reactor can be specially designed to address d-CaL applications: Ca-solid inputs close to ambient temperature, flue gas inputs at stack temperatures, minimum requirements of space and ancillary equipment and operation with maximum activity Ca-materials to minimize solid handling and transport cost. The carbonator reactor exploits known principles [45,46] developed for other applications of countercurrent reactor systems, including today's industrial shaft kilns, that use analogous materials and provide key similarities to facilitate the rapid scale up of the reactor proposed in this work.

2. Design of a countercurrent bed carbonator reactor for CO_2 capture with $CaO/Ca(OH)_2$

Fig. 1 shows a schematic representation of the countercurrent bed carbonator proposed in this work, plotted to highlight the mechanical similarities with existing shaft kilns for limestone calcination. The objective of the reactor is however just the opposite: instead of promoting the calcination of $CaCO_3$ stones or pebbles of 1–10 cm diameter in the central region of the reactor [47–51], here it is targeted the formation of $CaCO_3$ by the carbonation of Ca-solids (i.e. with active CaO or $Ca(OH)_2$ in the form of porous stones or pellets). As it will be discussed below, the countercurrent movement of gas and solids in the carbonator, together with the exothermic nature of the carbonation reaction facilitates the generation of a central region in the reactor at optimum carbonation temperatures of between 600 and 700 ℃. Decarbonized flue gases come out of such region and preheat the Ca-solids fed to the reactor at ambient temperature. On the other side, carbonated solids moving downwards to the exit of the reactor preheat the flue gas entering the reactor and moving upwards. This capability to integrate preheating and cooling steps in the reactor is a known feature of moving bed reactors such as shaft kilns and it has allowed them to reach high

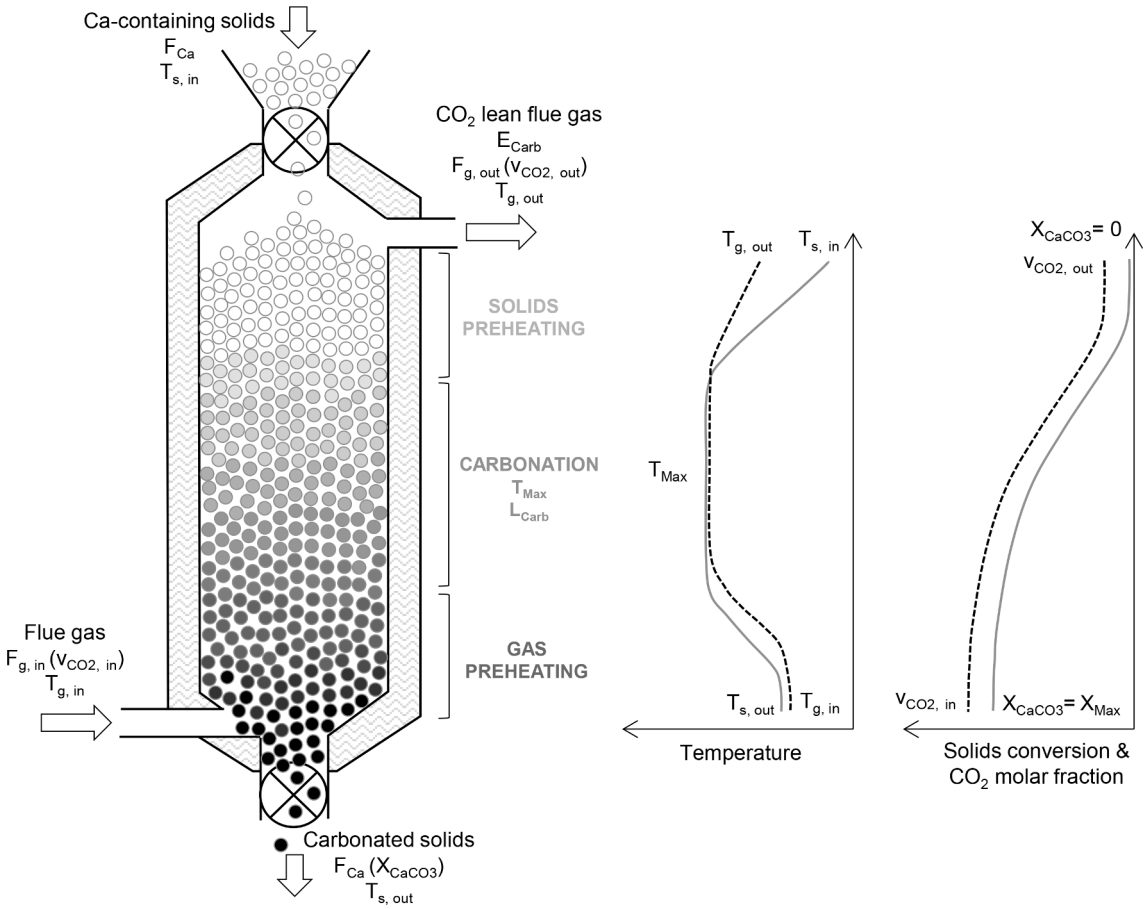

Fig. 1. Conceptual design of the moving bed carbonator reactor and qualitative profiles along the reactor length of the evolution of gas and solids temperatures (T_g and T_s), CO_2 molar fraction (v_{CO2}) and Ca solids conversion to $CaCO_3$ (X_{CaCO3}).

thermal efficiencies approaching the thermodynamic limits for calcination [49,51]. In d-CaL applications, as those reviewed in the Introduction section, the integration of solid preheating and cooling within the reactor will also be advantageous to minimize the footprint of the carbonator and the thermal inefficiencies.

By exploiting as much as possible the mechanical and thermal similarities with existing vertical shaft kilns, we can adopt a number of simplifying assumptions to facilitate basic design and investigate performance of this new carbonator reactor. As in lime kilns and in order to minimize the gas pressure drop in the moving bed when operating at superficial gas velocities of 1–3 m/s, the moving bed carbonator can deal with large stones of a few centimeters of characteristic size. With this range of particle size for the Ca-sorbent (especially when compared to the 100 μm average particle size used in fluidized bed carbonators [4,6,11,13,41] or the 10 μm used in entrained beds [42,52,53]), the rate of carbonation reaction will be typically very slow. It has been experimentally confirmed recently [54] that the carbonation rates of large Ca $(OH)_2$ forms (i.e., of 4 to 15 mm thickness) under a wide range of gas atmospheres (i.e., v_{CO2} from 0.0005 in air to up to 0.12) and temperatures from ambient to 800°C are controlled by the diffusion of CO_2 through the gas phase occupying the voids in the carbonated layer of the solids formed from the outside towards the inside of the particles.

A schematic representation of this model is shown in Fig. 2, together with indicative plots of conversion vs time curves. These have been calculated for different diameters (d_p) of CaO and $Ca(OH)_2$ particles, using the following equations for spherical pebbles with a constant average particle size:

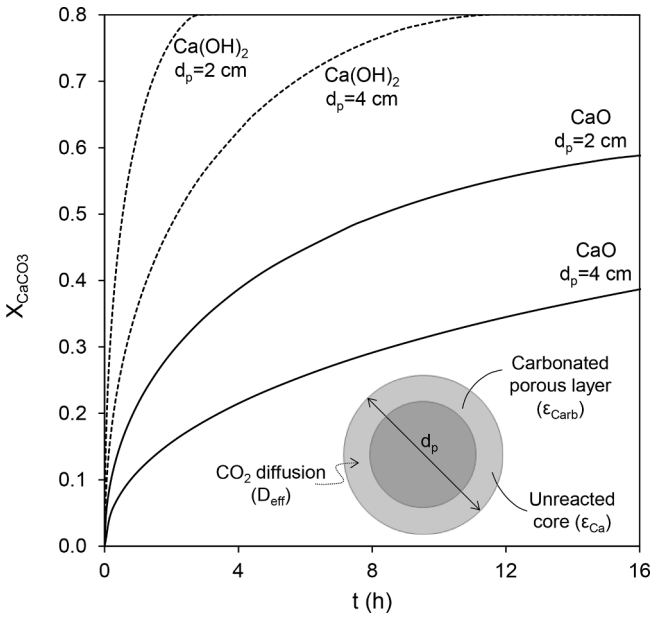

Fig. 2. Carbonation conversion of the Ca-sorbent (X_{CaCO3}) vs time (t) accordingly to the shrinking core model of equation (2) for spherical stones or pellets of CaO (full lines) and $Ca(OH)_2$ (dotted lines) with particles diameters (d_p) of 2 and 4 cm and ε_{Ca} = 0.5. Carbonation at 650 ℃ and a CO_2 molar fraction of 0.05.

$$\frac{dX_{CaCO3}}{dt} = \frac{3D_{eff}C_{CO2}}{\rho_{Ca,\ p}(d_p/2)^2}\frac{(1-X)^{1/3}}{1-(1-X)^{1/3}} \quad (1)$$

or in integrated form:

$$\frac{t}{\tau_R} = 1 - 3(1-X)^{2/3} + 2(1-X) \quad (2)$$

being τ_R

$$\tau_R = \frac{\rho_{Ca,\ p}(d_p/2)^2}{6D_{eff}C_{CO2}} \quad (3)$$

where X is the solid conversion with respect its total volume, D_{eff} is the effective diffusion of CO_2 through the carbonated layer, C_{CO2} the CO_2 concentration and $\rho_{Ca,\ p}$ the molar density of the porous particles with porosity ε_{Ca} (calculated as the product $\rho_{Ca}\bullet(1\text{-}\varepsilon_{Ca})$, being ρ_{Ca} the molar density of the Ca-solid). Since the process will be controlled by the CO_2 diffusion through the gas phase occupying the voids in the carbonated layer, D_{eff} has been calculated as $D_{CO2}\varepsilon_{Carb}/\tau$ where D_{CO2} is the CO_2 diffusion in air (as function the temperature and with a value of $1.13{\cdot}10^{-4}$ m^2/s at 650 ℃ [55]), ε_{Carb} the porosity of the carbonated layer and τ the tortuosity factor (calculated as $1/\sqrt{\varepsilon_{Ca}}$ [56]). The porosity of the carbonated layer is calculated by assuming that there is no expansion of the porous solid during carbonation and considering the maximum carbonation conversion of the Ca-sorbent as in equation (4). Taking into account the solid conversion with respect its total volume (X) and the molar active fraction of the Ca-solids ($f_{Ca,\ active}$) the carbonation conversion of the Ca-sorbent (X_{CaCO3}) is calculated as $X_{CaCO3} = X{\cdot}f_{Ca,\ active}$.

$$\varepsilon_{Carb} = 1 - (1 - X_{CaCO3})(1 - \varepsilon_{Ca}) - \frac{X_{CaCO3}\rho_{Ca}(1-\varepsilon_{Ca})}{\rho_{CaCO3}} \quad (4)$$

In equation (4) ρ_{Ca} and ρ_{CaCO3} are the molar densities of the Ca-solid (of 59.6 kmol/m^3 for CaO and 29.9 kmol/m^3 for $Ca(OH)_2$) and $CaCO_3$ (27.1 kmol/m^3).

As can be seen in the examples of Fig. 2, the time scales to reach carbonation conversions higher than 0.5 (assuming a molar active fraction of the Ca-solids $f_{Ca,\ active}$ of 0.6 for CaO and 0.8 for $Ca(OH)_2$ considering the higher reactivity for the $Ca(OH)_2$ resulting from the hydration of CaO [57]) span for several hours for stone sizes of 2 and 4 cm in diameter when carbonated at 650 ℃ in an atmosphere with an average CO_2 molar fraction of 0.05. In all cases, a porosity of $\varepsilon_{Ca} = 0.5$ has been assumed, being equivalent to ε_{Carb} of 0.14 and 0.46 for CaO and for $Ca(OH)_2$ respectively accordingly to equation (4). The superior porosity of the carbonated layer for $Ca(OH)_2$ solids compared to CaO enables for lower residence times or the possibility of more compact bed arrangements. In the case of CaO stones, there are constrains when considering the large difference in molar volume with respect to the $CaCO_3$ product layer. Therefore, CaO pebbles with $\varepsilon_{Ca} > 0.42$ are required to ensure $\varepsilon_{Carb} > 0$ and thus to avoid the reaction to stop due to pore plugging. Even if $\varepsilon_{Ca} = 0.44$, just 0.06 below the examples in Fig. 2, two orders of magnitude longer residence time (and hence reactor volume) would be required to achieve the same conversion. For such Ca-sorbents with limited porosity, it would be possible to moderate the pore plugging by reducing the activity of the material. However, this would translate into a less effective use of the solids, which is not optimum for d-CaL applications.

The long times scales shown in Fig. 2 (compared with time scales in the order of 10 s of seconds to 1 min when carbonating similar fine materials entrained or in fluidized beds [6,53,58–61]) indicates that the shrinking core model of equation (2) provides a suitable description of the progress of carbonation with time. This is again a comparable situation to what happens with the calcination reaction of similarly large scale stones in shaft kilns: despite the complexity of the $CaCO_3$ calcination process in short times and small microscopic scales, it has been well established [62] that calcining stones in the cm diameter range clearly follow a shrinking core model during calcination and typical residence times of solids in shaft kilns are usually chosen to be between 2 and 8 h to ensure complete calcination.

Under these conditions, with a slow motion of solids downwards in the reactor, very intense and effective heat transfer between the gas and the solids moving in countercurrent mode can be assumed, with the local temperature difference between gas and solids being negligible. This means that the axial temperature profile in the moving bed carbonator can be described in a simplified way as that presented in the middle of Fig. 1, that assumes an ideal regenerative heat exchange behavior of the solids preheating and cooling sections, which is close again to what is observed in practice in shaft kilns working under similar flow conditions and materials [47,48,50,63]. More advanced heat transfer models of the proposed countercurrent reactor will be required to analyze in detail other effects as, for example, the possible decoupling of the dehydration (endothermic reaction) and carbonation reactions (exothermic reaction) when $Ca(OH)_2$ is used as sorbent, or even a possible (re)hydration (exothermic reaction) of partially carbonated particles in the gas preheating zone when $H_2O_{(v)}$ present in the flue gas reacts with unconverted CaO. However, and for the sake of simplicity, these have been left outside the scope of this work.

In these conditions, it is possible to approximate the outlet gas temperature ($T_{g,\ out}$) and the maximum carbonation temperature reached in the central region of the reactor (T_{Max}) [45] from the mass and energy balances to the reactor. To this aim, the reactor it is assumed to operate under adiabatic conditions and only heat transfer between the gas and solid phases is taken into account. Also, as mentioned above, the temperature differences between the gas and solids in the carbonation zone are assumed to be negligible and the change in temperature between gas–solid heat exchange or preheating zones and carbonation zone is considered to take place in steps.

A first energy balance, summarized in equations (5) to (7), is used to calculate the outlet gas temperature ($T_{g,\ out}$) by assuming that $T_{g,\ in} = T_{s,\ out}$. Thus, for an adiabatic reactor,

$$(\text{Heat out}) - (\text{Heat in}) = (\text{Reaction heat}) \quad (5)$$

$$(q_{g,out} + q_{s,out}) - (q_{g,in} + q_{s,in}) = q_r \quad (6)$$

the outlet gas temperature ($T_{g,\ out}$) can be calculated as follows,

$$T_{g,\ out} = \frac{F_{g,\ in}Cp_{g,\ in}T_{g,\ in} + F_{s,\ in}Cp_{s,\ in}T_{s,\ in} - F_{s,\ out}Cp_{s,\ out}T_{s,\ out} + \left(\Delta H_{Carb}X_{CaCO3} + \Delta H_{Dehy}X_{Dehy}\right)F_{Ca}}{F_{g,\ out}Cp_{g,\ out}} \quad (7)$$

where F_i are the molar flows and Cp_i the molar specific heat (in J/molK) of each stream, ΔH_{Carb} the enthalpy of the CaO carbonation (i.e., 171 kJ/mol at 650 ℃), ΔH_{Dehy} the enthalpy of the $Ca(OH)_2$ dehydration (-104 kJ/mol at 500–600 °C), and X_{Dehy} the $Ca(OH)_2$ molar conversion to CaO. X_{Dehy} takes a value of 0 for CaO and 1 for $Ca(OH)_2$ considering that the $Ca(OH)_2$/CaO equilibrium allows for the dehydration of the particles at temperatures well below T_{Max} (being the equilibrium temperature around 520 ℃ under pure H_2O atmospheres [64]).

A second energy balance, summarized in equations (8) to (10), is used to calculate T_{Max} by including the $T_{g,\ out}$ from the first energy balance and assuming again that $T_{g,\ in} = T_{s,\ out}$, representing in this case

that the heat lost by the gas is totally gained by the solids.

$$(Heat\ gas\ out) - (Heat\ solids\ in) = (Heat\ gas\ \max) - (Heat\ solids\ \max) \tag{8}$$

$$q_{g,out} - q_{s,in} = q_{g,Max} - q_{s,Max} \tag{9}$$

$$T_{Max,ave} = \frac{F_{g,out}Cp_{g,out}T_{g,out} - F_{s,in}Cp_{s,in}T_{s,in}}{F_gCp_{g,Max} - F_sCp_{s,Max}} \tag{10}$$

To complete the heat balances above, the mass balances to the reactor need to be solved to calculate the sorbent requirements to achieve a certain CO_2 capture target. When adding the reaction kinetics (equations (1) to (4)), the CO_2 molar fraction and solids conversion profiles along the carbonation zone (as those qualitatively shown on the right-hand-side of Fig. 1) can be obtained to estimate the solids residence time and, thus, the required length of the carbonation zone (L_{Carb}). To this aim, a basic 1D reactor model has been developed by assuming that the conditions change only in the axial direction (z), with the radial dispersion being negligible. Plug flow is assumed for both the gas and solid phases in countercurrent mode and the gas phase is assumed to follow the ideal gas equation. Under countercurrent mode the boundary conditions taken are at $z = 0$, $C_{CO2} = C_{CO2,in}$ and $X = X_{exit}$ meanwhile at $z = L_{Carb}$, $C_{CO2} = C_{CO2,\ exit}$ and $X = 0$.

From the global mass balance to the CO_2 (equations (11) to (14)), the flow of Ca solids (F_{Ca}) with a maximum carbonation conversion of X_{CaCO3} are calculated for a certain CO_2 capture target (i.e. the ton of CO_2 capture per day of flue gas, F_g, with a molar fraction of CO_2, v_{CO2}, calculated as in equation (14)) and capture efficiency (E_{Carb}, as in equation (13)).

$$(mol\,CO_2)_{in} - (mol\,CO_2)_{out} = (mol\,CO_2)_{captured} = (mol\ Ca)_{reacts} \tag{11}$$

$$F_{CO2,in} - F_{CO2,out} = F_{Ca}\Delta X_{CaCO3} \tag{12}$$

$$E_{Carb} = 1 - \frac{F_{CO2,out}}{F_{CO2,in}} \tag{13}$$

$$\nu_{CO2} = \frac{F_{CO2}}{F_g} \tag{14}$$

$F_{CO2,\ in}$ and $F_{CO2,\ out}$ are the molar flow of CO_2 at the inlet and outlet of the reactor respectively and ΔX_{CaCO3} the variation of the solids Ca conversion to $CaCO_3$ along the reactor bed.

The evolution of the CO_2 concentration along the carbonation zone (z) can be calculated from the mass balance to the gas phase,

$$u_g\frac{dC_{CO2}}{dz} = \rho_{Ca,p}\frac{dX}{dt}(1-\varepsilon_B)f_{Ca\ active} \tag{15}$$

where u_g is the gas velocity and ε_B the bed porosity. Considering the reaction kinetics of equation (1), previous equation (15) can be rewritten as follows,

$$u_g\frac{dC_{CO2,\ z}}{dz} = \frac{3D_{eff}C_{CO2,z}}{(d_p/2)^2}\frac{(1-X_z)^{1/3}}{1-(1-X_z)^{1/3}}(1-\varepsilon_B)f_{Ca\ active} \tag{16}$$

where the solids conversion along the reactor (X_z) can be calculated as function of the CO_2 concentration as in equation (17) by taking into account the mass balance of equation (12) and considering that $F_{CO2} = C_{CO2}\cdot u_g\cdot A_B$ (being A_B the cross-sectional area of the reactor).

$$X_z = X_{out} - \frac{(C_{CO2,\ in} - C_{CO2,\ z})u_gA_B}{F_{Ca}f_{Ca\ active}} \tag{17}$$

By substituting equation (17) on equation (16), an integral without analytical solution is obtained.

$$\int_{C_{CO2,\ in}}^{C_{CO2}} \frac{1-\left(1-\left(X_{out}-\frac{(C_{CO2,\ in}-C_{CO2,\ z})u_gA_B}{F_{Ca}f_{Ca\ active}}\right)\right)^{\frac{1}{3}}}{C_{CO2,\ z}\left(1-\left(X_{out}-\frac{(C_{CO2,\ in}-C_{CO2,\ z})u_gA_B}{F_{Ca}f_{Ca\ active}}\right)\right)^{\frac{1}{3}}}dC_{CO2,\ z} = \int_{z=0}^{z=L_{Carb}} \frac{3D_{eff}}{(d_p/2)^2u_g}(1-\varepsilon_B)f_{Ca\ active}\ dz \tag{18}$$

Equation (18) can be numerically solved to obtain the total carbonation length (L_{Carb}) that fulfills the mass balances and the reaction kinetics considering the superficial velocity of the moving solids and thus their residence time, as in equation (19).

$$t_R = \frac{L_{Carb}(1-\varepsilon_B)A_B}{F_{Ca}\rho_{Ca,\ p}} \tag{19}$$

Fig. 3 shows the evolution of the CO_2 molar fraction and the Ca solids conversion to $CaCO_3$ along the carbonation zone. For illustrative purposes, the mass balances and kinetic equations above has been solved also for co-current movement of the gas and solids in the carbonator section (i.e. by taking into account that at $z = 0$, $C_{CO2} = C_{CO2,\ in}$ and $X = 0$ meanwhile at $z = L_{Carb}$, $C_{CO2} = C_{CO2,\ exit}$ and $X = X_{out}$) and assuming a constant temperature of 650 ℃. As it can be seen, the countercurrent gas–solid contact mode proposed allows for more compact reactors when maximizing the capture efficiency (i.e. $E_{Carb} = 0.9$). Under such high carbonation efficiencies, a co-current reactor about 3 times longer to that operated under countercurrent mode will be needed.

3. Operational windows to maximise CO_2 capture efficiencies and Ca-sorbent utilization

By solving the 1D reactor model equations noted in the previous section it is possible to select preferred operating windows of the proposed countercurrent carbonator. These, resulting from the combinations of inlet temperature, CO_2 concentration in the inlet gas and Ca-sorbent characteristics, will be governed by the need to achieve optimum temperatures in the central carbonation zone. In any case, these should target to maximize the Ca-sorbent utilization (i.e. $X_{CaCO3} > 0.5$) in order to minimize space requirements as well as solid handling and transport cost for d-CaL applications.

When using Ca-sorbents, the maximum CO_2 carrying capacity depends on first term on the reaction temperature [44,65,66]. $T_{Max} > 550$ ℃ is required to ensure fractions of active Ca material above 0.5. Contrary, T_{Max} is limited by the equilibrium curve of CO_2 on CaO, so that it cannot exceed the equilibrium temperature associated with the inlet CO_2 content of the flue gas, being the equilibrium CO_2 molar fraction ($v_{CO2,\ eq}$) rapidly increased from 0.01 at 610 ℃ up to 0.08 at 750 ℃. Thus, optimum carbonation temperatures should be around 600-650 ℃ in order to maximize the Ca-sorbent utilization (i.e. X_{CaCO3} of 0.6–0.8), while avoiding equilibrium restrictions in the carbonation zone.

When CaO is used as sorbent, it is well known that its CO_2 carrying capacity decay with the number of calcination-carbonation cycles due to a sintering effect [67]. This is not the case for $Ca(OH)_2$, as the introduction of a hydration step reverses this effect and produces a highly reactive sorbent every cycle [57,68,69]. Based on this, and for d-CaL applications capturing CO_2 from flue gases from external sources, two systems can be proposed in order to maximize the sorbent utilization, as shown in Fig. 4. On one side, and when CaO is used as sorbent, an open loop can be proposed (see left-hand-side of Fig. 4). This includes the use of freshly calcined limestone in the moving bed carbonator (i.e. from cycle one) and the subsequent oxy-calcination of the depleted sorbent to produce CO_2 for storage or use and CaO for the lime or cement industry where, for many applications, no constrains in terms of CO_2 carrying capacity exit. On the other side, and when using $Ca(OH)_2$ as sorbent, the scheme proposed is based on a closed loop (see right-hand-side of Fig. 4) where the depleted sorbent can be reused by introducing hydration and

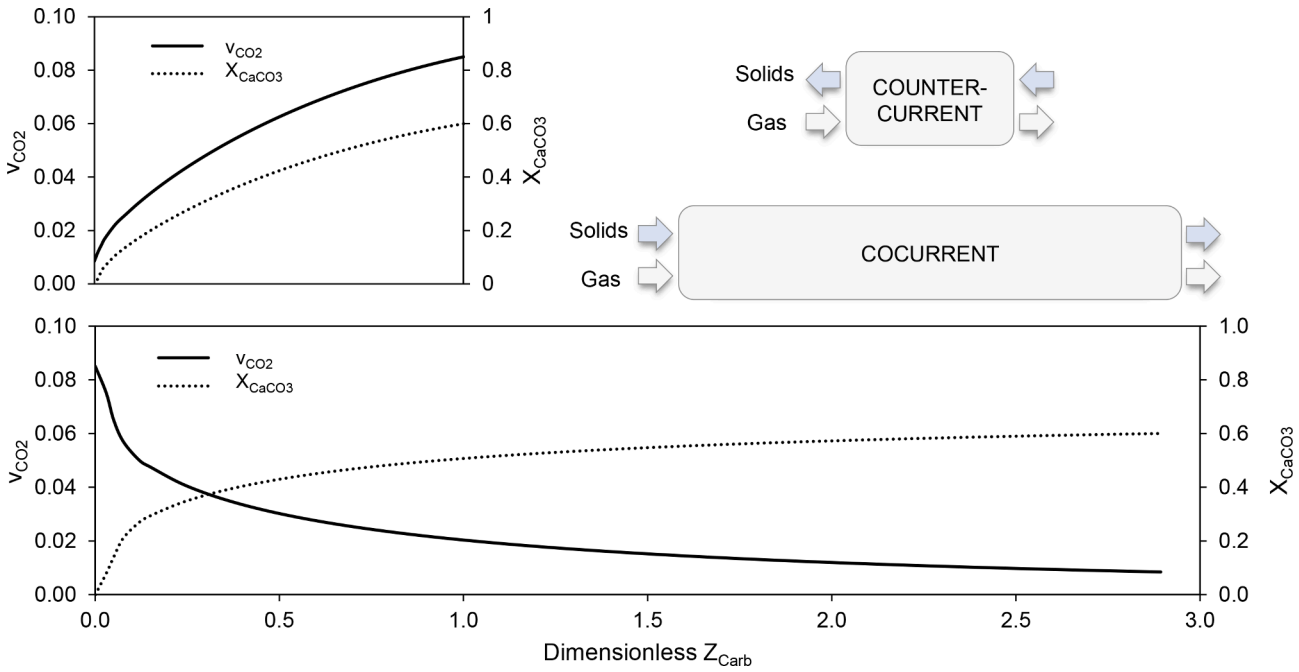

Fig. 3. Evolution of the CO_2 molar fraction (v_{CO2}) and Ca solids conversion to $CaCO_3$ (X_{CaCO3}) along the dimensionless countercurrent carbonation length ($Z_{Carb} = z/L_{Carb}$) for a gas–solid arrangement in countercurrent (top) and cocurrent (bottom) mode. Solved by assuming $E_{Carb} = 0.9$, $X_{CaCO3} = 0.6$, $v_{CO2,\ in} = 0.085$ and $T_{Max} = 650$ °C.

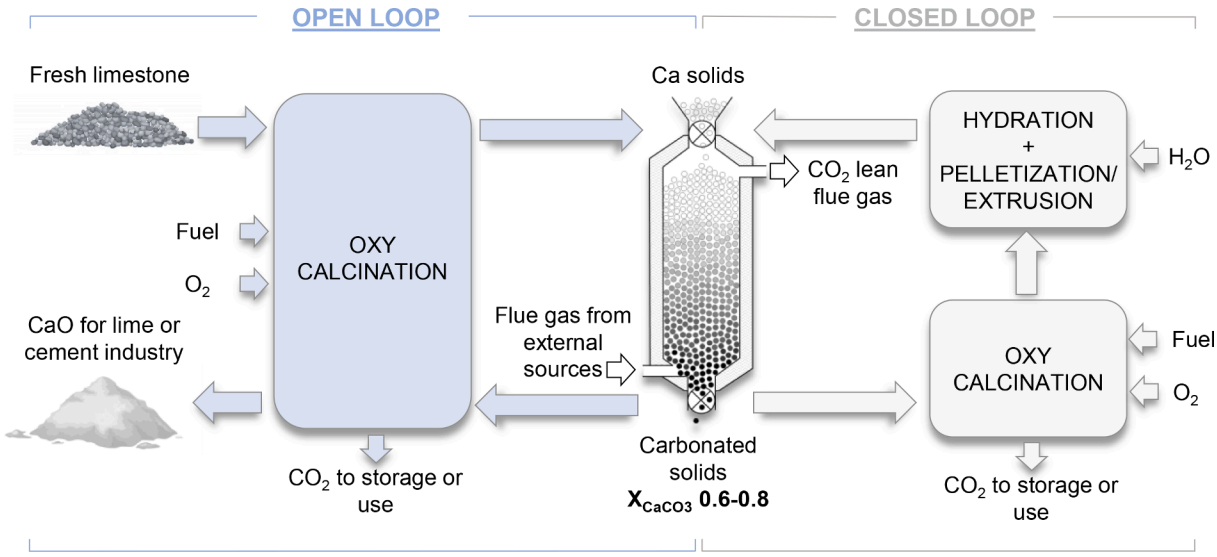

Fig. 4. Schematic representation of the two proposed d-CaL systems to maximize the utilisation of the Ca-sorbent by using fresh CaO (open loop, left) or $Ca(OH)_2$ obtained from the regenerated sorbent (closed loop, right).

shaping steps to manufacture $Ca(OH)_2$ pellets or extruded forms [54,70].

Feasible operational conditions can be found for the auto-thermally sustained reactor in order to ensure the optimum temperatures required for the carbonation. When a certain X_{CaCO3} is assumed, the T_{Max} as calculated from the mass and heat balances, will be function of the inlet gas temperature and CO_2 content. Thus, as the CO_2 molar fraction in the gas decreases, $T_{g,\ in}$ needs to be increased. Considering the heat balances of equations (5) to (10), optimum combinations of $T_{g,in}$ and $v_{CO2,in}$ can be found, as shown in Fig. 5a for a $T_{Max} = 650$ ℃ when considering a X_{CaCO3} of 0.6 and 0.8 for CaO and $Ca(OH)_2$ respectively and $E_{Carb} = 0.9$. Substantial differences can be found when using CaO or $Ca(OH)_2$ as result from the large differences in their reaction enthalpies (i.e. of 171 and 33 kJ/mol CO_2 respectively for CaO and $Ca(OH)_2$ at 650 C, with $X_{Dehy} = 1$ for $Ca(OH)_2$ and the respective X_{CaCO3} above noted). As can be seen in Fig. 5a, $v_{CO2,\ in}$ below 0.1 and 0.18 are required when using CaO and $Ca(OH)_2$, respectively. For CO_2 capture applications where $v_{CO2,\ in}$ is moderate (i.e. $v_{CO2,\ in}$ about 0.04–0.06) as in the case of flue gases produced in freight transport or in natural gas combustion, $T_{g,\ in}$ should be about 320-450 ℃ when using CaO as sorbent. These values increase up to 560–595 °C for $Ca(OH)_2$. For gases with very low CO_2 content (i.e. $v_{CO2,in} < 0.04$), $T_{g,\ in}$ approaches to T_{Max} and also the capture efficiency and the effectiveness of the reactor will be reduced as $v_{CO2,\ out} \approx v_{CO2,\ eq}$ at the reference T_{Max} of 650 ℃, thus resulting on increasing volumes of reactor at the equilibrium conditions (i.e. inactive for CO_2 capture).

It must be noted that the lines represented in Fig. 5a are not

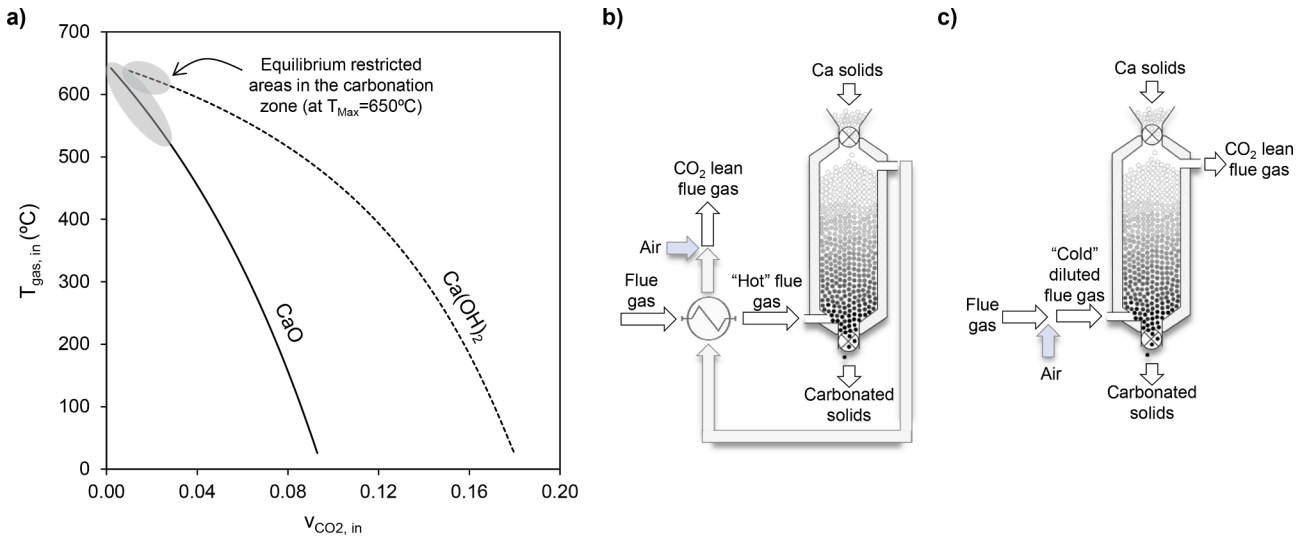

Fig. 5. a) Temperature of the inlet gas ($T_{g, in}$) required to ensure an auto-thermal carbonation zone at T_{Max} = 650 ℃ as a function of gas inlet CO_2 molar fraction ($v_{CO2, in}$) assuming an E_{Carb} = 0.9 and X_{CaCO3} of 0.6 and 0.8 for CaO and $Ca(OH)_2$, respectively, and X_{Dehy} = 1 for $Ca(OH)_2$. Possible arrangements of the scheme of Fig. 1 to adequate the gas conditions by **b)** increasing $T_{g, in}$ and **c)** decreasing $T_{g, in}$ and $v_{CO2,in}$.

restrictive for the applicability of the moving bed carbonator. For example, pairs of $T_{g, in}$ and $v_{CO2, in}$ values in between the two lines of Fig. 5a are feasible when using Ca-sorbents prepared as a mixtures of CaO and $Ca(OH)_2$. Such mixtures, with enthalpies in between 171 and 33 kJ/mol CO_2, allow for an additional freedom degree to reach T_{Max} = 650 ℃ in a wider range of inlet gas temperature and CO_2 molar fractions. In addition to this, and as schematically shown in Fig. 5b and c, different strategies can be proposed to adequate the inlet gas conditions. For example, for flue gases at mild temperatures and low CO_2 contents (i.e. $v_{CO2, in} < 0.08$, typical in energy efficient industrial processes) pre-heating the inlet gas using the outlet CO_2 lean flue gas in a gas–gas heat exchanger can be proposed (Fig. 5b) as in these cases $T_{g, out}$ is of between 530 and 600 ℃ for CaO and 460 and 620 ℃ for $Ca(OH)_2$, accordingly to equation (7). For flue gases at exceeding temperatures or CO_2 contents, the inlet flue gas can be mixed with ambient air to reduce the temperature of the product gas and/or to moderate the $v_{CO2, in}$, as schematically proposed in Fig. 5c. These are just illustrative situations, but other integration schemes can be as well proposed in order to stablish adequate input gas conditions that ensure optimized operational conditions for the moving bed carbonator.

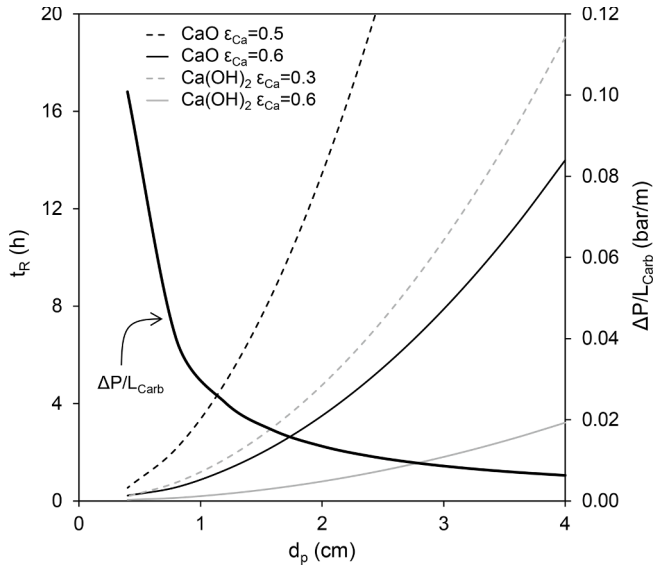

Fig. 6. Solids residence time (t_R) and pressure drop per length unit ($\Delta P/L_{Carb}$) as function of the Ca-sorbent diameter (d_p) for CaO (black lines) and $Ca(OH)_2$ (grey lines) of different ε_{Ca}. Plots for reference cases by assuming E_{Carb} = 0.9, X_{CaCO3} of 0.6 and 0.8 for CaO and $Ca(OH)_2$ respectively, $v_{CO2, in}$ = 0.085, T_{Max} = 650 ℃, $u_{gas, in}$ = 2 m/s (at 650 ℃) and ε_B = 0.4.

Based on the sorbent average particle size and internal porosity it is possible to calculate the residence time required to reach 90% of its maximum carbonation conversion (i.e., X = 0.9 and being X_{CaCO3} of 0.6 and 0.8 for CaO and $Ca(OH)_2$ respectively) accordingly to the reactor model described in the previous section including the axial concentration profiles of CO_2 in the gas. As shown in Fig. 6, there is a large margin to adapt the design of the reactor to the specific characteristic of the Ca-sorbent. For average d_p of between 1 and 2 cm and highly porous materials (i.e. ε_{Ca} about 0.6), the residence times are below 3.5 h as shown in Fig. 6. When using less porous materials (probably more representative of those available for large scale applications) the residence times increase up to values of between 2 and 13 h as shown in Fig. 6 for ε_{Ca} = 0.5 in the case of CaO pebbles (i.e. as obtained from the direct calcination of limestone) or 0.3 for extruded $Ca(OH)_2$.

Another outcome of the selection of the sorbent characteristics is the pressure drop along the reactor. Although in terms of reaction rates low particle sizes are favoured, the pressure drop per length unit sharply increases as d_p decreases. Accordingly to the Ergun's equation for fixed beds [71], pressure drops of between 0.03 and 0.01 bar/m are calculated for particle diameters of 1 and 2 cm (see Fig. 6) when considering typical gas velocities of 2 m/s and bed porosities (ε_B) of 0.4.

Finally, and to exemplify the proposed countercurrent moving bed, a reference case has been solved to capture 90% of the CO_2 present in a 3.9 m^3N/s flue gas stream with an inlet CO_2 molar fraction of 0.085, which is about 50 t_{CO2}/day. As discussed in Fig. 5a, $T_{g, in}$ of 109 and 500 C respectively are required to ensure a T_{Max} = 650 ℃ when using CaO or $Ca(OH)_2$ as sorbents with a X_{CaCO3} of 0.6 and 0.8 for CaO and $Ca(OH)_2$ respectively, being the outlet gas temperatures of 520 and 458 ℃. From the mass balance, the solids flow rate calculated are about 106 t/day. When assuming ε_{Ca} = 0.5 and 0.3 for respectively CaO and $Ca(OH)_2$ and average d_p of 1.5 cm, residence times of t_R = 7.6 and 2.7 h are calculated (see Fig. 6). For an average gas velocity of 2 m/s at 650 ℃ (0.6 m/s at standard normal conditions), the calculated cross-sectional area of the moving bed is of 6.5 m^2 and, applying equation (19), the length of the carbonation zone is of 5.1 and 2.0 m for CaO and $Ca(OH)_2$ respectively, resulting in a pressure drop in the carbonation zone of 40–100 mbar accordingly to Fig. 6.

In the absence of more detailed designs of the overall system involving the reactor and the solid storage silos, we can assume with the carbon balance the minimum volume requirements to store $Ca(OH)_2$ solids in silos. Assuming a bed porosity of 0.4, an internal porosity of the pellets of 0.35, and a maximum carbonation conversion of 0.8 at the exit of the moving bed carbonator reactor, a bed of $Ca(OH)_2$ will have a storage capacity of 10 kmolC/m^3, which can be compared for example with the carbon density in a diesel tank (about 60 kmolC/m^3) or a liquefied natural gas tank (about 30 kmolC/m^3).

The analysis of the feasible operational windows of the proposed countercurrent moving bed carbonator suggests that it is possible to ensure high CO_2 capture efficiencies using compact and highly thermal efficiency carbonator reactors decoupled from the sorbent regeneration. Further progress in these kind of reactors will be of special relevance for the deployment of d-CaL applications.

4. Conclusions

A moving bed carbonator reactor targeting for decoupled Calcium Looping applications has been presented as alternative to the conventional fluidized or bubbling beds. The requirements in terms of thermal efficiency and compactness for d-CaL systems are well reached by the proposed countercurrent carbonator moving bed using pebbles of CaO and/or extruded $Ca(OH)_2$ in the cm scale as CO_2 sorbent. The feeding of solids at ambient temperature while ensuring an auto-thermally maintained carbonation zone (thanks to the preheating of the inlet gas and solids streams with the outlet ones in countercurrent mode) will enable the solids handling and transport operations required for d-CaL systems. The high thermal efficiency of the proposed carbonator allows to capture CO_2 from a wide variety of flue gases. Although constrains in terms of input gas temperature and CO_2 molar fraction to fulfill the heat and mass balances in the reactor have been found, different strategies can be proposed to ensure optimized carbonation temperatures around 600-700 ℃ (as for example using $CaO/Ca(OH)_2$ mixtures, preheating the inlet gas using the outlet CO_2 lean flue gas or even diluting the flue gas). Such reaction temperatures will ensure a maximum sorbent utilization (i.e. X_{CaCO3} are about 0.6–0.8 when using CaO from freshly calcined limestone or pellets or extruded of $Ca(OH)_2$ produced from hydrated CaO) as to both minimize the cost of solids handling and transport operations and moderate the reactor size. In addition to this, the countercurrent operation mode also ensures compact reactor designs with high capture efficiencies (i.e. of 90%), being the required reactor lengths about 3 times smaller when compared to cocurrent mode. For Ca-sorbents of 1 to 2 cm of diameter, the reaction will be governed by the CO_2 diffusion through the carbonated layer. Based on this, the reaction times calculated are of between 2 and 13 h for materials with modest porosity (i.e. 0.5 for CaO and 0.3 for $Ca(OH)_2$) and the pressure drop per reactor length of between 0.01 and 0.03 bar/m when operated under typical gas velocities of 2 m/s. These operational conditions are in the range of what is standard in existing shaft kilns, what will help to scale up the technology.

Declaration of Competing Interest

The authors declare the following financial interests/personal relationships which may be considered as potential competing interests: Juan Carlos Abanades Garcia has patent #CO_2 capture method using an autothermal countercurrent moving bed carbonator - Application number EP21382947.6 pending to Consejo Superior de Investigaciones Científicas (CSIC). Yolanda Alvarez Criado has patent #CO_2 capture method using an autothermal countercurrent moving bed carbonator - Application number EP21382947.6 pending to Consejo Superior de Investigaciones Científicas (CSIC).

Data availability

Data will be made available on request.

Acknowledgements

This research has been developed within the CSIC Interdisciplinary Thematic Platform (PTI+) Transición Energética Sostenible+ (PTI-TRANSENER+) as part of the CSIC program for the Spanish Recovery, Transformation and Resilience Plan funded by the Recovery and Resilience Facility of the European Union, established by the Regulation (EU) 2020/2094. The authors also acknowledge the financial support provided by the European Union under the Research Fund for Coal and Steel (RFCS) Program (BackCap Project, GA 10103400).

References

[1] T. Shimizu, T. Hirama, H. Hosoda, K. Kitano, M. Inagaki, K. Tejima, A twin fluid-bed reactor for removal of CO_2 from combustion processes, Chem. Eng. Res. Des. 77 (1999) 62–68, https://doi.org/10.1205/026387699525882.
[2] B. Arias, M.E. Diego, J.C. Abanades, M. Lorenzo, L. Diaz, D. Martínez, J. Alvarez, A. Sánchez-Biezma, Demonstration of steady state CO_2 capture in a 1.7 MWth calcium looping pilot, Int. J. Greenh. Gas Control. 18 (2013) 237–245, https://doi.org/10.1016/j.ijggc.2013.07.014.
[3] B. Arias, M.E. Diego, A. Méndez, M. Alonso, J.C. Abanades, Calcium looping performance under extreme oxy-fuel combustion conditions in the calciner, Fuel. 222 (2018) 711–717, https://doi.org/10.1016/j.fuel.2018.02.163.
[4] J. Ströhle, J. Hilz, B. Epple, Performance of the carbonator and calciner during long-term carbonate looping tests in a 1 MWth pilot plant, J. Environ. Chem. Eng. 8 (2020), 103578, https://doi.org/10.1016/j.jece.2019.103578.
[5] J.C. Abanades, B. Arias, A. Lyngfelt, T. Mattisson, D.E. Wiley, H. Li, M.T. Ho, E. Mangano, S. Brandani, Emerging CO_2 capture systems, Int. J. Greenh. Gas Control. 40 (2015) 126–166, https://doi.org/10.1016/j.ijggc.2015.04.018.
[6] I. Martínez, G. Grasa, J. Parkkinen, T. Tynjälä, T. Hyppänen, R. Murillo, M. C. Romano, Review and research needs of Ca-Looping systems modelling for post-combustion CO_2 capture applications, Int. J. Greenh. Gas Control. 50 (2016) 271–304, https://doi.org/10.1016/j.ijggc.2016.04.002.
[7] USGS, Crushed stone statistics and information, (2022). https://www.usgs.gov/centers/nmic/crushed-stone-statistics-and-information (accessed December 2022).
[8] EULA, European Lime Association, (2022). https://www.eula.eu/ (accessed December 2022).
[9] IEA, Cement, International Energy Agency, Paris, 2021. https://www.iea.org/reports/cement (accessed December 2022).
[10] J. Blamey, E.J. Anthony, J. Wang, P.S. Fennell, The calcium looping cycle for large-scale CO_2 capture, Prog. Energy Combust. Sci. 36 (2010) 260–279, https://doi.org/10.1016/j.pecs.2009.10.001.
[11] J.C. Abanades, Calcium looping for CO_2 capture in combustion systems, Woodhead Publ. Ser. Energy, Woodhead Publishing, 2013, pp. 931–970, https://doi.org/10.1533/9780857098801.4.931.
[12] M.E. Boot-Handford, J.C. Abanades, E.J. Anthony, M.J. Blunt, S. Brandani, N. Mac Dowell, J.R. Fernández, M.-C. Ferrari, R. Gross, J.P. Hallett, R.S. Haszeldine, P. Heptonstall, A. Lyngfelt, Z. Makuch, E. Mangano, R.T.J. Porter, M. Pourkashanian, G.T. Rochelle, N. Shah, J.G. Yao, P.S. Fennell, Carbon capture and storage update, Energy Environ. Sci. 7 (2014) 130–189, https://doi.org/10.1039/C3EE42350F.
[13] D.P. Hanak, E.J. Anthony, V. Manovic, A review of developments in pilot-plant testing and modelling of calcium looping process for CO_2 capture from power generation systems, Energy Environ. Sci. 8 (2015) 2199–2249, https://doi.org/10.1039/C5EE01228G.
[14] A. Perejón, L.M. Romeo, Y. Lara, P. Lisbona, A. Martínez, J.M. Valverde, The Calcium-Looping technology for CO_2 capture: On the important roles of energy integration and sorbent behavior, Appl. Energy. 162 (2016) 787–807, https://doi.org/10.1016/j.apenergy.2015.10.121.
[15] M. Bui, C.S. Adjiman, A. Bardow, E.J. Anthony, A. Boston, S. Brown, P.S. Fennell, S. Fuss, A. Galindo, L.A. Hackett, J.P. Hallett, H.J. Herzog, G. Jackson, J. Kemper, S. Krevor, G.C. Maitland, M. Matuszewski, I.S. Metcalfe, C. Petit, G. Puxty, J. Reimer, D.M. Reiner, E.S. Rubin, S.A. Scott, N. Shah, B. Smit, J.P.M. Trusler, P. Webley, J. Wilcox, N. Mac Dowell, Carbon capture and storage (CCS): the way forward, Energy Environ. Sci. 11 (2018) 1062–1176, https://doi.org/10.1039/C7EE02342A.
[16] N. Rodríguez, R. Murillo, J.C. Abanades, CO_2 capture from cement plants using oxyfired precalcination and/or Calcium Looping, Environ. Sci. Technol. 46 (2012) 2460–2466, https://doi.org/10.1021/es2030593.
[17] D.C. Ozcan, H. Ahn, S. Brandani, Process integration of a Ca-looping carbon capture process in a cement plant, Int. J. Greenh. Gas Control. 19 (2013) 530–540, https://doi.org/10.1016/j.ijggc.2013.10.009.
[18] M.C. Romano, M. Spinelli, S. Campanari, S. Consonni, M. Marchi, N. Pimpinelli, G. Cinti, The Calcium Looping process for low CO_2 emission cement plants, Energy Procedia. 61 (2014) 500–503, https://doi.org/10.1016/j.egypro.2014.11.1158.
[19] K. Atsonios, P. Grammelis, S.K. Antiohos, N. Nikolopoulos, E. Kakaras, Integration of calcium looping technology in existing cement plant for CO_2 capture: Process

modeling and technical considerations, Fuel. 153 (2015) 210–223, https://doi.org/10.1016/j.fuel.2015.02.084.
[20] E. De Lena, M. Spinelli, I. Martínez, M. Gatti, R. Scaccabarozzi, G. Cinti, M. C. Romano, Process integration study of tail-end Ca-Looping process for CO_2 capture in cement plants, Int. J. Greenh. Gas Control. 67 (2017) 71–92, https://doi.org/10.1016/j.ijggc.2017.10.005.
[21] M. Voldsund, S.O. Gardarsdottir, E. De Lena, J.-F. Pérez-Calvo, A. Jamali, D. Berstad, C. Fu, M. Romano, S. Roussanaly, R. Anantharaman, H. Hoppe, D. Sutter, M. Mazzotti, M. Gazzani, G. Cinti, K. Jordal, Comparison of technologies for CO_2 capture from cement production—Part 1: Technical evaluation, Energies. 12 (2019) 559. https://www.mdpi.com/1996-1073/12/3/559.
[22] Cleanker, Clean clinker by Calcium Looping for low-CO_2 cement, (2022). www.cleanker.eu (accessed December 2022).
[23] IPCC, Climate change 2022 - Mitigation of climate change. Summary for policymakers, Working Group III contribution to the Sixth Assessment Report of the Intergovernmental Panel on Climate Change, 2022.
[24] J. Alcalde, N. Heinemann, L. Mabon, R.H. Worden, H. de Coninck, H. Robertson, M. Maver, S. Ghanbari, F. Swennenhuis, I. Mann, T. Walker, S. Gomersal, C. E. Bond, M.J. Allen, R.S. Haszeldine, A. James, E.J. Mackay, P.A. Brownsort, D. R. Faulkner, S. Murphy, Acorn: Developing full-chain industrial carbon capture and storage in a resource- and infrastructure-rich hydrocarbon province, J. Clean. Prod. 233 (2019) 963–971, https://doi.org/10.1016/j.jclepro.2019.06.087.
[25] T.A. Meckel, A.P. Bump, S.D. Hovorka, R.H. Trevino, Carbon capture, utilization, and storage hub development on the Gulf Coast, Greenh. Gases, Sci. Technol. 11 (2021) 619–632, https://doi.org/10.1002/ghg.2082.
[26] European Comission - Climate Action, Reducing emissions from the shipping sector, (2022). https://ec.europa.eu/clima/eu-action/transport-emissions/reducing-emissions-shipping-sector_en (accessed December 2022).
[27] J.A. Ros, E. Skylogianni, V. Doedée, J.T. van den Akker, A.W. Vredeveldt, M.J. G. Linders, E.L.V. Goetheer, J.-G.-M.-S. Monteiro, Advancements in ship-based carbon capture technology on board of LNG-fuelled ships, Int. J. Greenh. Gas Control. 114 (2022), 103575, https://doi.org/10.1016/j.ijggc.2021.103575.
[28] Seabound - We capture CO_2 emissions from ships, (2022). https://www.seabound.co/ (accessed December 2022).
[29] Calix, RECAST - A system to decarbonise long-distance shipping, (2022). https://www.calix.global/co2-mitigation-focus-area/recast-a-system-to-decarbonise-long-distance-shipping/ (accessed December 2022).
[30] B.N.C. Sweeney, System to reduce CO_2 emissions from shipping and heavy transport, GB 2527608 A, 2014.
[31] P. Renforth, B.G. Jenkins, T. Kruger, Engineering challenges of ocean liming, Energy. 60 (2013) 442–452, https://doi.org/10.1016/j.energy.2013.08.006.
[32] K.S. Lackner, P. Grimes, H.J. Ziock, Capturing carbon dioxide from air, in: First Natl. Conf. Carbon Sequestration, Washington, DC, 2001.
[33] S. Elliott, K.S. Lackner, H.J. Ziock, M.K. Dubey, H.P. Hanson, S. Barr, N. A. Ciszkowski, D.R. Blake, Compensation of atmospheric CO_2 buildup through engineered chemical sinkage, Geophys. Res. Lett. 28 (2001) 1235–1238, https://doi.org/10.1029/2000GL011572.
[34] P. Renforth, The negative emission potential of alkaline materials, Nat. Commun. 10 (2019) 1401, https://doi.org/10.1038/s41467-019-09475-5.
[35] J.C. Abanades, Y.A. Criado, J.R. Fernández, An air CO_2 capture system based on the passive carbonation of large $Ca(OH)_2$ structures, Sustain, Energy Fuels. 4 (2020) 3409–3417, https://doi.org/10.1039/D0SE00094A.
[36] 8 Rivers Capital - Calcite Removal, (2022). https://8rivers.com/portfolio/calcite/ (accessed December 2022).
[37] A. Goff, D. Beauchamp, J.E. Fetvedt, M.R. Palmer, X. Lu, D. Rathbone, Direct capture of carbon dioxide, WO 2021/111366 A1, 2021.
[38] J.C. Abanades, Y.A. Criado, CO_2 capture method using a countercurrent moving bed reactor, Application number EP21382947.6, 2021.
[39] J.C. Abanades, Y.A. Criado, Method of capturing CO_2 from the atmosphere and air contactor device configured to carry out the method of capturing CO_2, Application number EP22382686 (2022).
[40] P. Lisbona, R. Gori, L.M. Romeo, U. Desideri, Techno-economic assessment of an industrial carbon capture hub sharing a cement rotary kiln as sorbent regenerator, Int. J. Greenh. Gas Control. 112 (2021), 103524, https://doi.org/10.1016/j.ijggc.2021.103524.
[41] N. Rodríguez, M. Alonso, J.C. Abanades, Experimental investigation of a circulating fluidized-bed reactor to capture CO_2 with CaO, AIChE J. 57 (2011) 1356–1366, https://doi.org/10.1002/aic.12337.
[42] M. Spinelli, I. Martínez, M.C. Romano, One-dimensional model of entrained-flow carbonator for CO_2 capture in cement kilns by Calcium looping process, Chem. Eng. Sci. 191 (2018) 100–114, https://doi.org/10.1016/j.ces.2018.06.051.
[43] M. Fantini, M. Spinelli, CLEANKER Overview, in: ECRA/CEMCAP/CLEANKER Work. 2018 Carbon Capture Technol. Cem. Ind., Brussels, 17 October 2018, n.d.
[44] Y.A. Criado, B. Arias, J.C. Abanades, Effect of the carbonation temperature on the CO_2 carrying capacity of CaO, Ind. Eng. Chem. Res. 57 (2018) 12595–12599, https://doi.org/10.1021/acs.iecr.8b02111.
[45] G. Eigenberger, Fixed bed reactors, in: Ullmann's Encycl. Ind. Chem. Vol B4, VCH - Verlag, Weinheim, Germany, 1992: pp. 199–238.
[46] G.F. Froment, K.B. Bischoff, Chemical reactor analysis and design, New York, 1979.
[47] A. Schmid, H. Hofer, Method for carrying out endothermic processes in a shaft furnace, US 3.074.706, 1963.
[48] E. Füssl, Regenerative shaft furnace for burning carbonate-containing raw materials, US 4.382.779, 1983.
[49] J.A.H. Oates, Lime and limestone: Chemistry and technology, production and uses, Wiley-VCH, Weinheim (1998), https://doi.org/10.1002/9783527612024.
[50] H. Piringer, Lime Shaft Kilns, Energy Procedia. 120 (2017) 75–95, https://doi.org/10.1016/j.egypro.2017.07.156.
[51] R.S. Boynton, Chemistry and technology of lime and limestone, 2 nd, John Wiley & Sons, New York, 1980.
[52] J. Plou, I. Martínez, G.S. Grasa, R. Murillo, Experimental carbonation of CaO in an entrained flow reactor, React, Chem. Eng. 4 (2019) 899–908, https://doi.org/10.1039/C9RE00015A.
[53] B. Arias, Y.A. Criado, B. Pañeda, J.C. Abanades, Carbonation kinetics of $Ca(OH)_2$ under conditions of entrained reactors to capture CO_2, Ind. Eng. Chem. Res. 61 (2022) 3272–3277, https://doi.org/10.1021/acs.iecr.1c04888.
[54] Y.A. Criado, J.C. Abanades, Carbonation rates of dry $Ca(OH)_2$ mortars for CO_2 capture applications at ambient temperatures, Ind. Eng. Chem. Res. 61 (2022) 14804–14812, https://doi.org/10.1021/acs.iecr.2c01675.
[55] E.N. Fuller, P.D. Schettler, J.C. Giddings, New method for prediction of binary gas-phase diffusion coefficients, Ind. Eng. Chem. 58 (1966) 18–27, https://doi.org/10.1021/ie50677a007.
[56] D.A.G. Bruggeman, Calculation of different physical constants of heterogeneous substances I: Dielectric constant and conductivity of media of isotropic substances, Ann. Phys. Ser. 24 (1935) 636–644.
[57] N. Phalak, W. Wang, L.-S. Fan, $Ca(OH)_2$-based Calcium Looping process development at The Ohio State University, Chem. Eng. Technol. 36 (2013) 1451–1459, https://doi.org/10.1002/ceat.201200707.
[58] G. Grasa, R. Murillo, M. Alonso, J.C. Abanades, Application of the random pore model to the carbonation cyclic reaction, AIChE J. 55 (2009) 1246–1255, https://doi.org/10.1002/aic.11746.
[59] Z. Li, H. Sun, N. Cai, Rate equation theory for the carbonation reaction of CaO with CO_2, Energy & Fuels. 26 (2012) 4607–4616, https://doi.org/10.1021/ef300607z.
[60] C. Ortiz, J.M. Valverde, R. Chacartegui, L.A. Perez-Maqueda, Carbonation of limestone derived CaO for thermochemical energy storage: From kinetics to process integration in concentrating solar plants, ACS Sustain. Chem. Eng. 6 (2018) 6404–6417, https://doi.org/10.1021/acssuschemeng.8b00199.
[61] Z. Li, General rate equation theory for gas–solid reaction kinetics and its application to CaO carbonation, Chem. Eng. Sci. 227 (2020), 115902, https://doi.org/10.1016/j.ces.2020.115902.
[62] C.C. Furnas, The rate of calcination of limestone, Ind. Eng. Chem. 23 (1931) 534–538, https://doi.org/10.1021/ie50257a017.
[63] B. Krause, B. Liedmann, J. Wiese, P. Bucher, S. Wirtz, H. Piringer, V. Scherer, 3D-DEM-CFD simulation of heat and mass transfer, gas combustion and calcination in an intermittent operating lime shaft kiln, Int. J. Therm. Sci. 117 (2017) 121–135, https://doi.org/10.1016/j.ijthermalsci.2017.03.017.
[64] I. Barin, Thermochemical data of pure substances, VCH Verlagsgesellschaft Weinheim, Germany, 1989.
[65] Z. Li, F. Fang, X. Tang, N. Cai, Effect of temperature on the carbonation reaction of CaO with CO_2, Energy & Fuels. 26 (2012) 2473–2482, https://doi.org/10.1021/ef201543n.
[66] V. Manovic, E.J. Anthony, Carbonation of CaO-based sorbents enhanced by steam addition, Ind. Eng. Chem. Res. 49 (2010) 9105–9110, https://doi.org/10.1021/ie101352s.
[67] R. Barker, The reversibility of the reaction $CaCO_3 \rightleftarrows CaO+CO_2$, J. Appl. Chem. Biotechnol. 23 (1973) 733–742, https://doi.org/10.1002/jctb.5020231005.
[68] I. Martínez, G. Grasa, R. Murillo, B. Arias, J.C. Abanades, Evaluation of CO_2 carrying capacity of reactivated CaO by hydration, Energy & Fuels. 25 (2011) 1294–1301, https://doi.org/10.1021/ef1015582.
[69] F.-C. Yu, N. Phalak, Z. Sun, L.-S. Fan, Activation strategies for calcium-based sorbents for CO_2 capture: A perspective, Ind. Eng. Chem. Res. 51 (2011) 2133–2142, https://doi.org/10.1021/ie200802y.
[70] Talleres Felipe Verdés S.A., (2022). https://www.verdes.com/ (accessed on October 2022).
[71] R.B. Perry, D.W. Green, Perry's Chemical Engineers' Handbook, McGraw-Hill, 1999.